Original Article

Effect of Suramin on Renal Proximal Tubular Cells Damage Induced by Cisplatin in Rats (Histological and Immunohistochemical Study)

Eman Ali El-Kordy[1,2]

[1]Department of Histology, Faculty of Medicine, Tanta University, Tanta, Egypt, [2]Department of Anatomy, College of Medicine, Imam Mohammad Ibn Saud Islamic University, Riyadh, Saudi Arabia

Abstract

Background: Renal toxicity is the most common complication of cispaltin therapy that has broad-spectrum antitumor activity against a variety of human solid tumor. Suramin, a Food and Drug Administration-approved old drug is a polysulfonated compound of napthylurea originally designed to treat trypanosomiasis. **Aim:** The current work aimed to investigate the possible protective effect of different doses of suramin against cisplatin-induced renal proximal tubular cells (RPTCs) damage. **Material and Methods:** Fifty adult male rats were used and divided into five equal groups. Group I served as a control, group II received suramin alone (10 mg/kg). Groups III, IV and V were administered cisplatin once (5 mg/kg, intraperitoneally) alone or combined with low dosage suramin (5 mg/kg) or high dosage suramin (10 mg/kg) once intravenously respectively. **Results:** Compared with control rats, cisplatin administration caused proximal tubules damage, RPTCs vacuolation with pyknotic nuclei, loss of brush border and widespread caspase-3 immunostaining. Cisplatin-induced RPTCs toxicity was further confirmed morphometrically (a significantly decreased proximal tubular epithelium height and increased mean number of caspase-3-immunopositive cells). These changes were accompanied by biochemical alteration manifested as a significant increase of blood urea nitrogen and serum creatinine. Simultaneous administration of high-dose but not low-dose suramin to the cisplatin-treated rats improved the deleterious morphological and morphometrical effects on RPTCs and restored the aforementioned biochemical parameters to control values. **Conclusion:** In conclusion suramin in a dose dependant manner protects RPTCs from damage induced by cisplatin.

Keywords: Cisplatin renal toxicity, histopathology, proximal tubules, suramin

Introduction

Cancer continues to be the world's largest cause of death. In 2018, the World Health Organization reported that cancer was the second leading cause of death with an estimated 9.6 million deaths worldwide.[1] Cisplatin (cis-diammine-dichloro-platinum) is one of the most effective chemotherapy agents that has broad-spectrum antitumor activity against a variety of human solid tumors.[2-4] Renal toxicity is the most common complication of cispaltin therapy that limits its clinical uses accounting for about 30% of hospitalized patients.[5-7] Cisplatin is metabolized in renal proximal tubular cells (RPTCs) to its nephrotoxic metabolite which develops mainly in the S3 segment 48–72 h after its administration.[8-10]

Received: 20.04.2019 **Revised:** 16.05.2019
Accepted: 22.05.2019 **Published:** 18.11.2019

Access this article online

Quick Response Code:

Website: http://www.jmau.org/

DOI: 10.4103/JMAU.JMAU_21_19

The exact mechanism of cisplatin-induced RPTCs damage has not been fully elucidated. However, several biological responses, including mitochondrial dysfunction, activation of cell death pathways, generation of reactive oxygen metabolites (ROM) and a robust inflammatory response resulting in RPTCs death by apoptosis and necrosis have been involved in playing an important roles in cisplatin-induced renal toxicity.[10,11]

Suramin, a Food and Drug Administration-approved drug is a polysulfonated compound of napthylurea originally designed

Address for correspondence: Dr. Eman Ali El- Kordy, Department of Histology, Faculty of Medicine, Tanta University, Tanta, Egypt.
E-mail: dr.emanelkordy@gmail.com

How to cite this article: El-Kordy EA. Effect of suramin on renal proximal tubular cells damage induced by cisplatin in rats (histological and immunohistochemical study). J Microsc Ultrastruct 2019;7:153-64.

in 1920 to treat trypanosomiasis as well as infections of Onchocerca volvulus.[12] Research interest in this old drug has turned in recent years to a new use. Several studies have recently shown that suramin protects animal models against muscle and liver fibrosis as well as reduces brain and kidney injury caused by ischemia reperfusion in rodents.[13,14] In addition, delayed suramin administration was also effective in mitigating renal fibrosis progression in obstructive nephropathy and in attenuating liver injury following exposure to D-galactosamine and lipopolysaccharide in mice.[12-15]The mechanisms by which suramin protects these organs from injury are linked to apoptosis inhibition, inactivation of nuclear factor-kB and reduction of toxic proinflammatory cytokine formation as tumor necrotic factor α (TNF-α).[14,16]

However, the studies of suramin effect as renoprotective agent on cisplatin treated animals induced RPTCs damage are very limited. Based on these, we examined in the current study the possible protective effect of different doses of suramin on histological, immunohistochemical and morphometrical RPTCs changes of cisplatin treated rats and correlated these effects with blood urea nitrogen and serum creatinine levels.

Materials and Methods

Animals

The experiment was conducted on 50 adult male albino rats, 8 weeks of age (180–200 g) that were housed in temperature and humidity controlled conditions under a light/dark photocycle with food and water supplied *ad libitum*. Ethical animal treatment protocols were followed, Tanta Faculty of Medicine.

Chemicals

Cisplatin was obtained as a vial of 10 mg/10 ml saline (Unistin; EIMC United Pharmaceuticals, Badr city, Cairo, ARE). Suramin was purchased from Sigma Aldrich (St. Louis, MO), each 100 mg was dissolved in 10 ml saline (10 mg/ml). All other chemicals used in the experiment were of analytical grade. Suramin was administered by tail vein injection while cisplatin intraperitoneally.

Experiment design

After 2 weeks of acclimatization, rats were classified into 5 groups, 10 rats each.

- Group I (control group): Was subdivided into two subgroups, five animals were left untreated, whereas the others were given a single intravenous injection (tail vein) of 1 ml saline
- Group II (suramin group): Were administered a single dose of suramin (10 mg/kg)[17]
- Group III (cisplatin treated group): Were injected with a single dose of cisplatin (5 mg/kg)[18,19]
- Group IV (low dosage suramin treated group) and Group V (high dosage suramin treated group): Rats were injected with cisplatin as in group III and were concomitantly given a single suramin dosage (5 mg/kg) or (10 mg/kg) respectively 2 h after cisplatin injection.

All rats were sacrificed under ether inhalation after 3 days from the beginning of the experiment, Histological, immunohistochemical, morphometrical and biochemical studies were conducted.

Histological and immunohistochemical study

Fresh small pieces from the right renal cortex were taken, fixed in 10% buffered formalin and processed for examination by light microscopy to gain (5–7 im) sections of paraffin to be stained with:[20-22]

1. Hematoxylin and eosin (H and E)
2. Periodic acid Schiff method (PAS)
3. Immunohistochemical staining using avidinngstoche peroxidase system to detect caspase-3. For detection of apoptosis, paraffin sections of 5 μm thickness had been stained with modified avidineds, par peroxidase for caspase-3.The primary antibodies used were monoclonal anticaspase-3 mouse (Thermo Fisher Scientific Inc., Rockford, Illinois, USA) at 1:100 dilution, which incubated at room temperature with slides for 1 h. Then, the sections were counterstained with Meyerer hematoxylin. Caspase-3 marker shows brown cellular cytoplasmic localization in early apoptosis and brown nuclear localization in late apoptosis.

For transmission electron microscope (TEM), thin slices of the left renal cortex were immediately fixed in 2.5% phosphate-buffered glutaraldehyde (pH 7.4), post fixed in 1% cold osmium tetroxide for 2 h in the same buffer at 4°C, dehydrated and embedded in epoxy resin. Sections of ultrathin (50–80 nm) were stained with uranyl acetate and lead citrate[23] for examination by (JEM-1010) transmission electron microscopy (TEM; Jeol, Tokyo, Japan) in Tanta University Electron Microscopy Unit.

Morphometrical study

The image analyzer computer system Leica Qwin 500 (England) in the Central laboratory, Faculty of Medicine, Tanta University was used to evaluate:

1. Proximal tubular epithelial height and proximal tubular diameter in hematoxylin and eosin-stained sections (×400)
2. Number of caspase-3 immunopositive cells per low power field.

The data were then collected in an Excel sheet and submitted to statistical analysis.

Biochemical study

At time of sacrifice, venous blood samples from all animals were obtained from the retro-orbital sinus, collected in heparinized tubes and centrifuged at 3000 rpm for 15 min. The serum was stored at-20°C until it was assayed for following biochemical parameters:[24]

1. Blood urea nitrogen (BUN)
2. Serum creatinine (SCr)

All performed procedures were strictly in accordance with a commercially available spectrophotometric enzymatic kit (Thermo Trace BECGMAN, Germany).

Statistical analysis

Statistical analysis were performed using SPSS program, version 17 (IBM Corporation, Somers, New York, USA) in the form of mean (X) ± standard deviation. Differences between the groupsn means were assessed using a one-way analysis of variance. P <0.05 was considered to be statistically significant.

Results

Histological and immunohistochemical results

Control and suramin groups (Groups I and II)

Renal cortex sections of both control subgroups and suramin group showed the same histological structure. Sections stained with H and E showed renal corpuscles, proximal convoluted tubules (PCTs) and distal convoluted tubules. The PCTs constituted the main bulk of the cortex, their cells (RPTCs) had narrow lumina and cuboidal acidophilic cells containing rounded vesicular nuclei with prominent nucleoli [Figure 1a and b].

Regarding PAS reaction, renal cortex sections revealed a PAS-positive reaction along the prominent apical brush borders of the RPTCs as well as at their basement membrane [Figure 2].

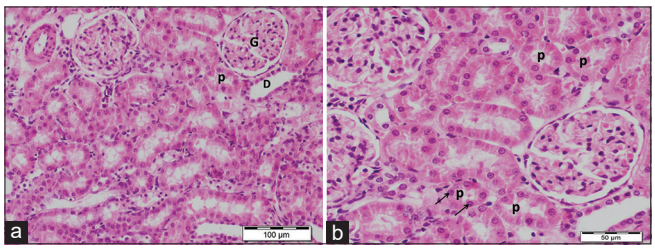

Figure 1: (a and b) Proximal convoluted tubules (p) have narrow lumina, acidophilic cuboidal cells containing round vesicular nuclei with prominent nucleoli (arrows). G, a renal corpuscle containing glomerulus and D, a distal convoluted tubule. Renal cortex of control rat H and E, (a) scale bar 100 µm and (b) scale bar 50 µm

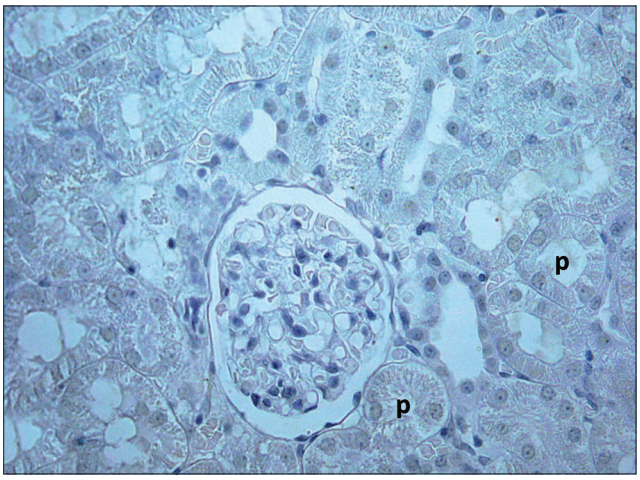

Figure 3: Proximal convoluted tubules (p) with negative immunoreactivity for caspase-3 of RPTCs. Renal cortex of control rat Caspase-3 immunostaining ×400

Caspase-3 immunostained sections, demonstrated negative staining of the RPTCs [Figure 3].

Ultrastructurally, RPTCs showed profuse long closely packed apical microvilli with multiple vesicles immediately beneath it. Their cytoplasm had numerous elongated moderately dense mitochondria with lamellar cristae arranged perpendicular on the trilamellar basal lamina and the nuclei were large, basal and euchromatic. The RPTCs were observed to be joined by junctional complexes along the apical part of the lateral cell boundaries together with narrow intercellular space [Figure 4a-c].

Cisplatin treated group (group III)

H and E-stained renal cortex sections of cisplatin treated rats showed obvious histological changes affecting most of the PCTs that appeared destroyed with areas of disorganization

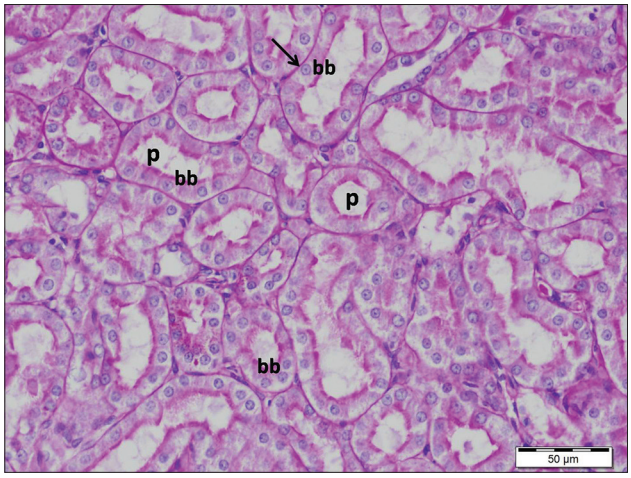

Figure 2: Proximal convoluted tubules (p) with PAS-positive reaction along apical brush border (bb) of RPTCs and continuous clear basement membrane (arrow). Renal cortex of control rat, PAS, scale bar 50 µm

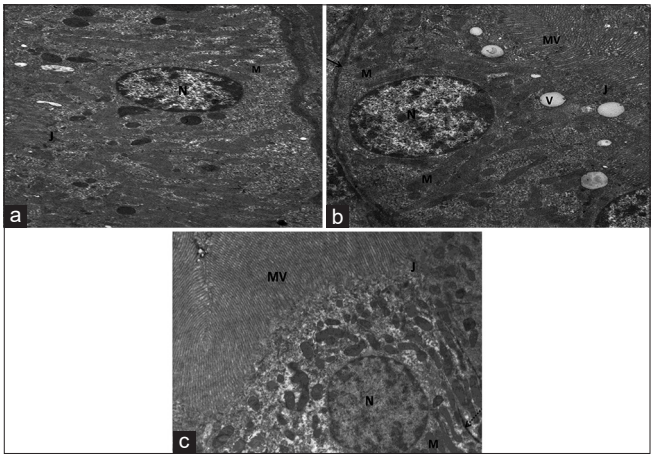

Figure 4: (a-c) Renal proximal tubular cells show profuse long apical microvilli (MV), elongated abundant mitochondria (m) arranged perpendicular on trilamillar basal lamina (arrow), multiple vesicles (v) and euchromatic nuclei (n). Note intercellular space (dotted arrow) and junctional complexes (j). Renal cortex of control rat TEM, (a) ×1000, (b) ×1500 and (c) ×2500

and loss of cellular architecture. RPTCs exhibited vacuolated cytoplasm with pyknotic densely stained nuclei and others appeared separated from their basement membrane. Some tubules appeared with widened irregular lumina comprising dense acidophilic hyaline casts as well as shedding and desquamation of lining epithelium. Interstitial mononuclear cellular infiltration as well as interstitial hemorrhage were also observed [Figures 5a, b and 6].

PAS-stained sections revealed RPTCs with an apparent weak disrupted reaction at their brush border and prominent positive reaction of the basement membrane that appeared thickened in many area and interrupted at other sites. In addition, some PCTs appeared with evident complete loss PAS reaction at the brush border and others with positively stained hyaline casts in the lumina surrounded by strong positive PAS membrane [Figure 7a and b].

Regarding caspase-3 immunostained sections, there was widespread brown staining of most RPTCs with intensive expression in exfoliated cells [Figure 8].

The electron micrographs of renal cortex of cisplatin treated rats showed remarkable changes in the proximal tubular cells, most of the cells exhibited marked vacuolated cytoplasm contained vacuolated mitochondria with destroyed cristae and multiple heterogeneous vacuoles studded with electron dense particles [Figures 9a-c and 10]. Other RPTCs exhibited marked loss of their mitochondria in rarefied cytoplasm leaving empty spaces and the remaining mitochondria were small in size with electron dense matrix [Figure 11].Their nuclei appeared dark shrunken heterochromatic with irregular nuclear envelope and dilated perinuclear space, Moreover apical displacement of the nuclei was observed [Figures 10 and 11]. Some RPTCs appeared with interrupted basal lamina, meanwhile others showed focal thickening and splitting of these lamina [Figures 9a-c and 10]. In addition, widening of intercellular spaces as well as distortion and focal loss of microvilli were observed [Figures 10 and11].

Low dosage suramin treated group (group IV)

By H and E stain, renal cortex sections of low dosage suramin treated rats showed the similar changes as those in group III.

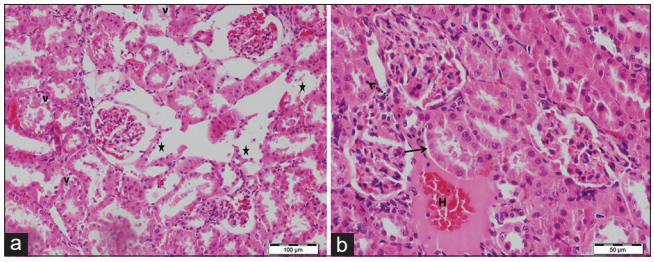

Figure 5: (a and b) Marked destruction and disorganization of most PCTs with loss of normal architecture (stars), proximal tubular cells with vacuolated cytoplasm (v) and small pyknotic nuclei (dotted arrow). Note RPTCs separation from basement membrane (arrow) and interstitial hemorrhage (h). Renal cortex of cisplatin treated rat H and E, (a) scale bar 100 μm and (b) scale bar 50 μm

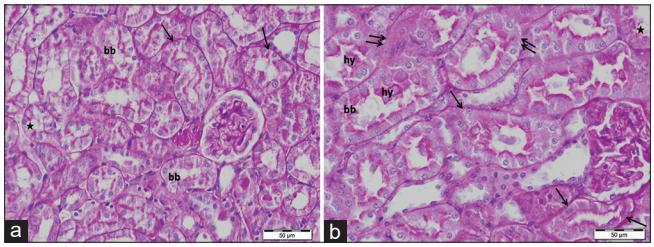

Figure 7: (a and b) RPTCs with an apparent weak disrupted PAS- positive reaction brush border (bb), strong positive reaction of thickening basement membrane (arrows) with interrupted one in many areas (double arrows). Note some PCTs with evident complete loss PAS reaction at the brush border (stars) and positively stained hyaline casts in tubular lumina (hy). Renal cortex of cisplatin treated rat PAS, (a and b) scale bar 50 μm

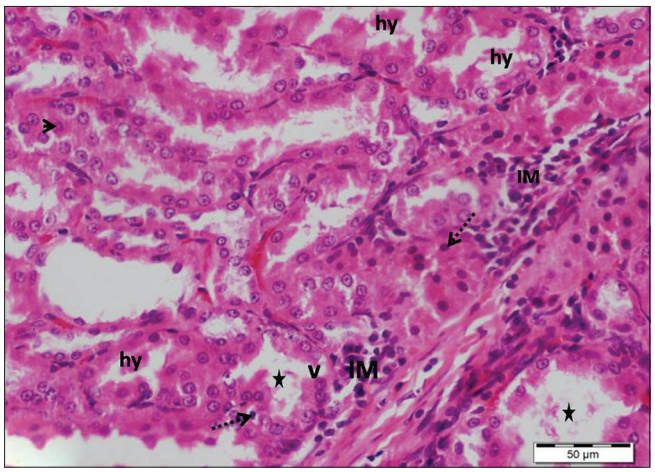

Figure 6: Marked degenerative changes of PCTs, some exhibit irregular dilated lumina (stars) comprising dense acidophilic hyaline casts (hy), RPTCs with vacuolated cytoplasm (v) and small pyknotic nuclei (dotted arrows), shaded epithelium (arrow head) and interstitial mononuclear cellular infiltration (IM). Renal cortex of cisplatin treated rat H and E, scale bar 50 μm

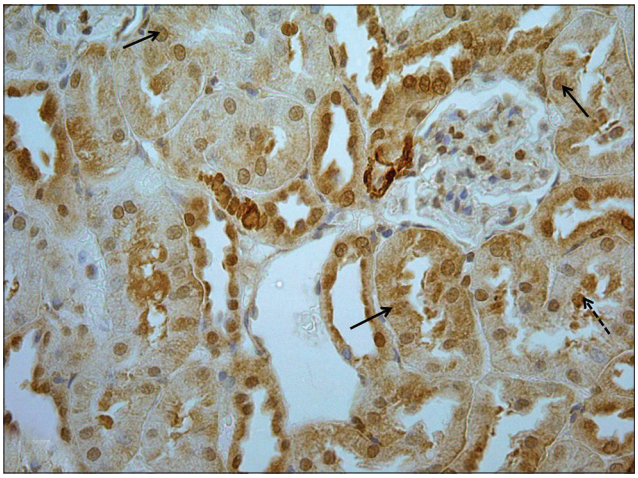

Figure 8: Widespread brown immunoreactivity for caspase-3 of most proximal tubular cells (arrows) with intensive expression in exfoliated cells (dotted arrow). Renal cortex of cisplatin treated rat Caspase-3 immunostaining ×400

The PCTs were still affected with dilated lumina. Most RPTCs appeared with marked cytoplasmic vacuolation and small pyknoic nuclei. Shedding epithelium and separated cells from their basement membrane were also observed [Figure 12a and b].

Regardless, few RPTCs displayed normal PAS-positive reaction along the apical brush border, most cells had still an apparent weak interrupted PAS-positive brush border with strong positive reaction of the basement membrane [Figures 13a and b].

Immunohistochemical reactions revealed marked brown immunoreaction for caspase-3 of most RPTCs and only a few one displayed weak reaction [Figure 14].

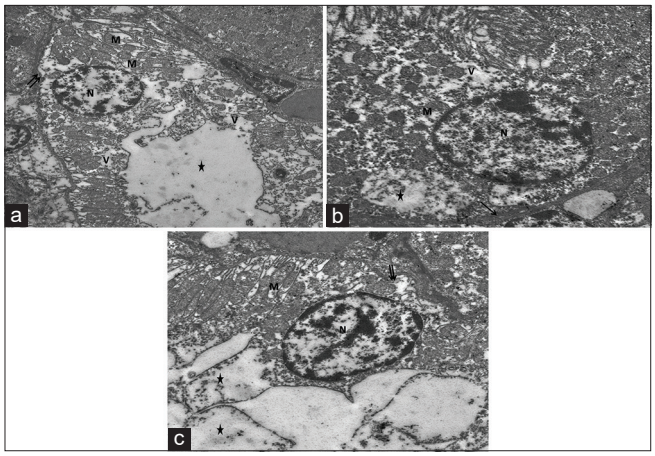

Figure 9: (a-c) Proximal tubular cells show vacuolated cytoplasm (v) contains vacuolated mitochondria with destructed cristae (m) and interrupted basal lamina (double arrows) meanwhile its focal thickening in other sites (arrow). Stars, rarified cytoplasm with remnants of cytoplasmic components and N, nucleus. Renal cortex of cisplatin treated rat TEM, (a) ×1000, (b) ×1500 and (c) ×2500

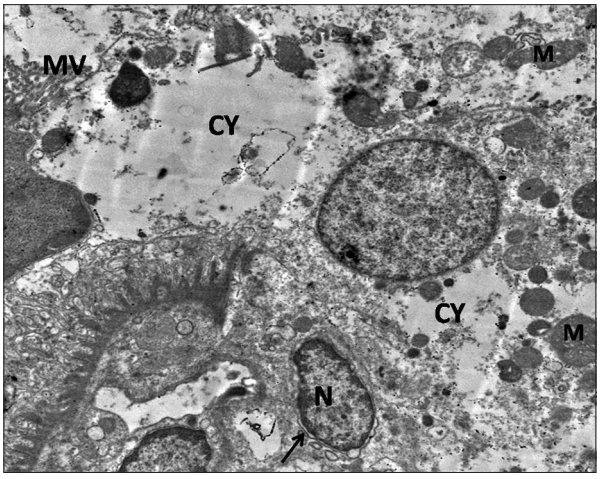

Figure 11: Proximal tubular cells show rarefied cytoplasm (CY) contains small sized disorganized electron dense mitochondria (M) and small irregular heterchromatic nucleus (N) with dilated perinuclear space (arrow). Note a few distorted microvilli (MV). Renal cortex of cisplatin treated rat TEM, ×2500

The electron micrographs confirmed the results observed by light microscope as no obvious improvement in the RPTCs. Most cells were still affected and appeared with electron dense irregular arrangement different shaped mitochondria in disrupted cytoplasm, small dark heterochromatic nuclei and widening intercellular spaces as well as focal loss of microvilli [Figure 15]. Moreover, multiple lysosomes and vacuoles in the cytoplasm of some cells were seen [Figure 16]. Few RPTCs appeared with normal euchromatic nuclei [Figure 17].

High dosage suramin treated group (group V)

H and E stained renal cortex sections of high dosage suramin treated rats, showed partial improvement in the histological structure of the PCTs which appeared more or less normal. Most RPTCs appeared with acidophilic cytoplasm and rounded vesicular nuclei, while some one showed cytoplasmic vacuolation with pyknotic nuclei [Figure 18a and b].

PAS-stained sections revealed preserved intact brush border and continuous clear basement membrane of most RPTCs, while a few one appeared with weak interrupted brush border [Figure 19a and b].

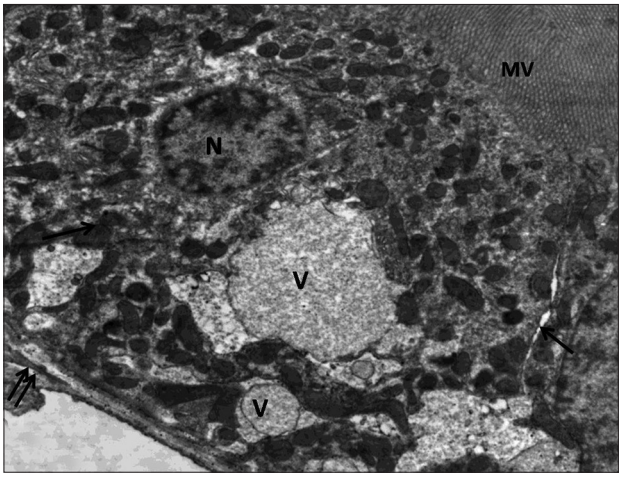

Figure 10: Proximal tubular cells show heterogenous irregular multiple cytoplasmic vacuoles (V), apical displacement of small heterchromatic nucleus (N), focal splitting of basal lamina (double arrows) and dilated intercellular space (arrow). MV, microvilli. Renal cortex of cisplatin treated rat TEM, ×2500

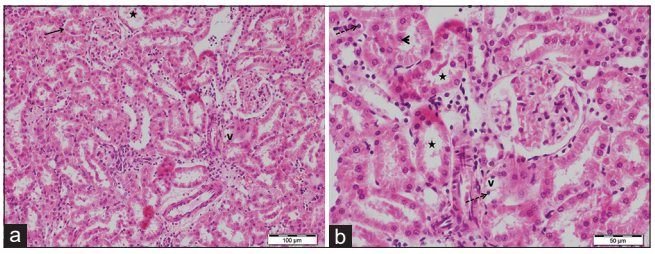

Figure 12: (a and b) Degenerated PCTs with dilated lumina (stars), RPTCs with vacuolated cytoplasm (v), small pyknoic nuclei (dotted arrows), shedding epithelium (arrow head) and others separated from their basement membrane (arrow). Renal cortex of low dosage suramin treated rat H and E, (a) scale bar 100 μm and (b) scale bar 50 μm

Regarding the immunohistochemistry, most RPTCs were observed with weak immunoreactivity for caspase-3 in comparison to cisplatin treated rats. Otherwise, a few one appeared with brown reactions [Figure 20].

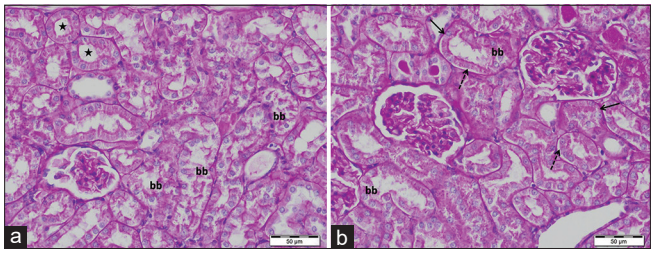

Figure 13: (a and b) Most RPTCs have an apparent weak interrupted PAS- positive brush border (bb) and strong positive reaction of the basement membrane (arrows). Note a few PCTs with more or less normal intact brush border of their cells (stars). Dotted arrows, RPTCs with detached basement membrane. Renal cortex of low dosage suramin treated rat PAS, (a and b) scale bar 50 μm

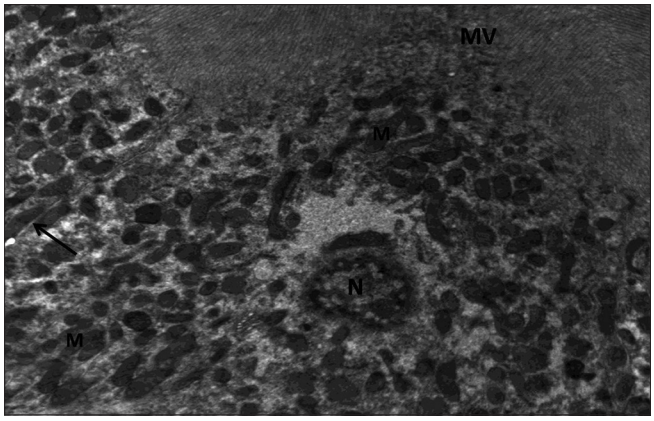

Figure 15: Proximal tubular cells show electron dense different sized and shaped disoriented mitochondria (M), a shrunken heterchromatic nucleus (N) and disrupted focal loss microvilli (MV). Note dilated intercellular spaces (arrow). Renal cortex of low dosage suramin treated rat TEM, ×2500

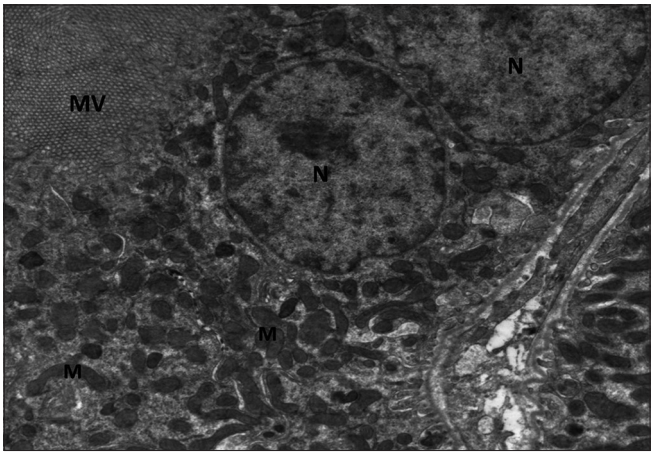

Figure 17: Proximal tubular cells with normal euchromatic nuclei (N) and electron dense mitochondria (M). MV, microvilli. Renal cortex of low dosage suramin treated rat TEM, ×2500

Ultrastructurally, RPTCs showed large euchromatic nuclei and numerous intact elongated mitochondria perpendicular to trilamellar basal lamina with minimal vacuolation of the cytoplasm. Restoration of the long apical microvilli was observed as well as preserved junctional complexes with narrow intercellular space [Figure 21a and b]. However, some

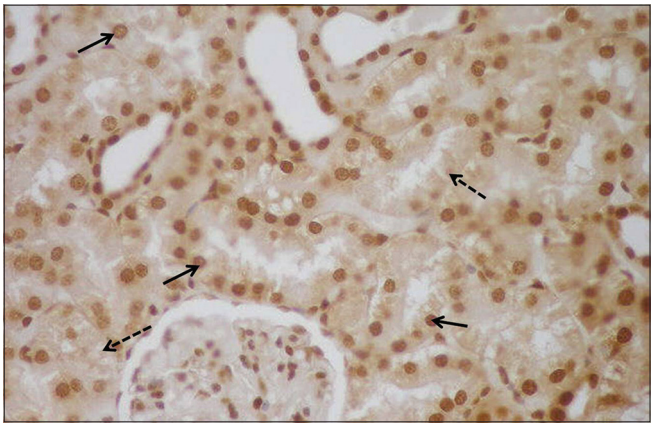

Figure 14: Most RPTCs have brown nuclear immunoreaction for caspase-3 (arrows) and a few one displayed weak reaction (dotted arrows). Renal cortex of low dosage suramin treated rat Caspase-3 immunostaining ×400

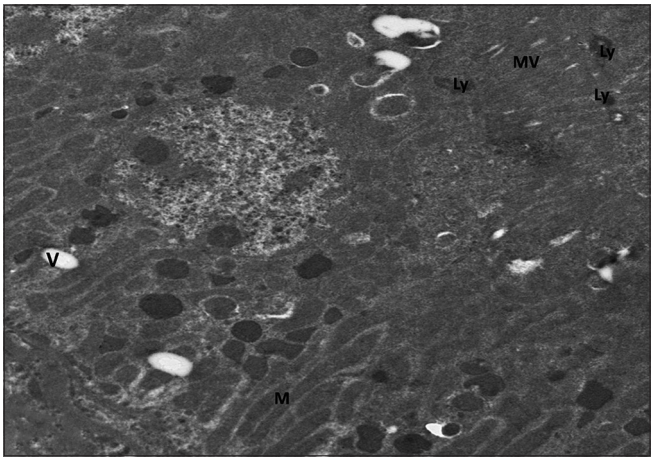

Figure 16: Proximal tubular cells with multiple lysosomes (Ly) and vacuoles (V). Note elongated mitochondria (M) and microvilli (MV). Renal cortex of low dosage suramin treated rat TEM, ×2000

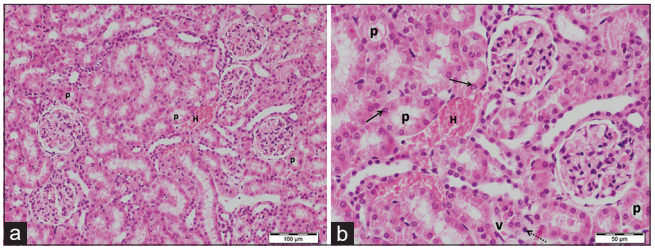

Figure 18: (a and b) An apparent normal PCTs (P), have more or less normal cells with vesicular nuclei (arrows). Note a few RPTCs with vacuolated cytoplasm (v) and pyknotic nuclei (dotted arrow). H, interstitial hemorrhage. Renal cortex of high dosage suramin treated rat H and E, (a) scale bar 100 μm and (b) scale bar 50 μm

cells were still affected and had irregular shaped electron dense mitochondria and dark shrunken heterochromatic nuclei [Figure 22].

Morphometric results

As shown in Table 1 and Graphs 1, 2, cisplatin treated rats (group III) had a significantly decreased proximal tubular epithelium height and a significantly increased proximal tubular diameter as compared to control animals ($P < 0.05$). Treating rats with low dosage suramin (group IV) did not show significant changes in both parameters while high dosage suramin treated rats (group V) had a significantly increased proximal tubular epithelium height and a significantly decreased proximal tubular diameter ($P < 0.05$) as compared to cisplatin group. However, no significant change ($P > 0.05$) was observed in both aforementioned parameters in the suramin alone treatment group (group II) as compared to control one.

The mean number of caspase-3-immunopositive cells for all groups is presented in Table 2 and Graph 3. There was a significant increase ($P < 0.05$) in cisplatin group (group III) as compared to the control one that remained significantly high in low dosage treated rats (group IV). A statistically significant decrease ($P < 0.05$) in the number of caspase-3-immunopositive cells was observed in rats treated with high dosage suramin (group V) compared with group III. This parameter was nonsignificant different ($P > 0.05$) in suramin group (group II) in comparison to the control.

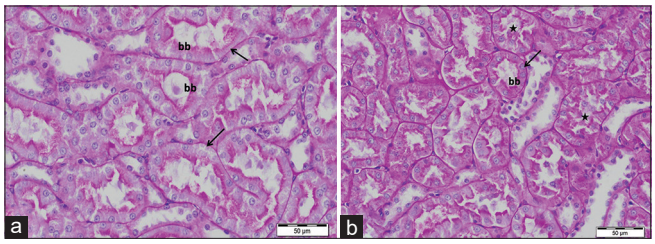

Figure 19: (a and b) Most RPTCs appear with preserved intact brush border (bb) and continuous clear basement membrane (arrows). Note a few PCTs with weak interrupted brush border (stars). Renal cortex of high dosage suramin treated rat PAS (a and b) scale bar 50 μm

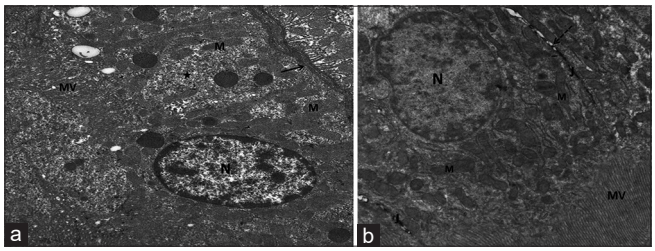

Figure 21: (a and b) Proximal tubular cells show euchromatic nuclei (N) and numerous intact mitochondria (M) with minimal cytoplasmic vacuolation (star). Note microvilli (MV), trilamillar basal lamina (arrow) and preserved junctions (J) with narrow intercellular space (dotted arrow). Renal cortex of high dosage suramin treated rat TEM, (a) ×1500, (b) ×2500

Biochemical results

As shown in Table 3 and Graphs 4 and 5, cisplatin treated rats (group III) had a high significantly increased levels of BUN and SCr as compared to control animals ($P < 0.05$). Treating rats with low dosage suramin (group IV) did not

Table 1: Proximal tubular epithelium height and proximal tubular diameter (μm) in control and experimental groups

Groups	Proximal tubular epithelial cells height (μm)	Proximal tubular diameter (μm)
Group I	10.23±0.928	28.23±4.608
Group II	10.12±0.691	24.98±3.792
Group III	3.45±0.559[a]	54.65±6.139[a]
Group IV	5.74±0.811	48.9±4.578
Group V	8.61±0.513[b]	34.84±3.996[b]

Values are expressed as mean±SD. [a]$P<0.05$ as compared to control, [b]$P<0.05$ as compared to cisplatin group. SD: Standard deviation

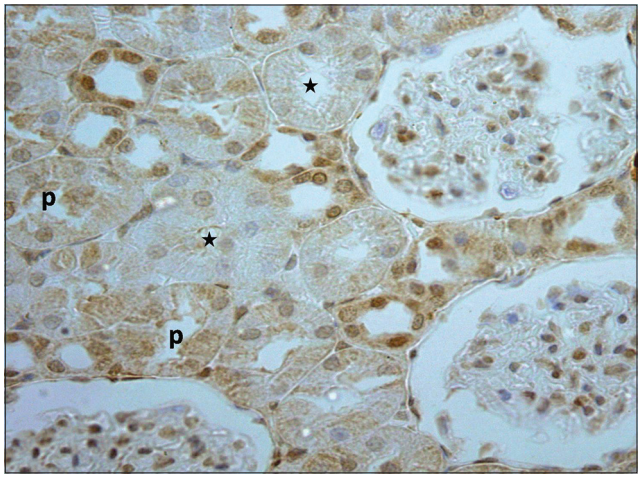

Figure 20: PCTs with an appearing weak immunoreactivity for caspase-3 of their cells (stars). Note a few tubules with brown immunoreactions (P). Renal cortex of high dosage suramin treated rat Caspase-3 immunostaining ×400

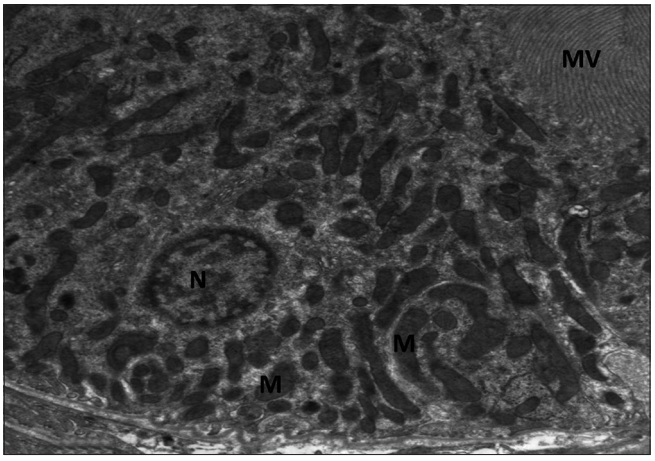

Figure 22: Proximal tubular cells with irregular shaped electron dense mitochondria and a small heterochromatic nucleus (N). MV, microvilli. Renal cortex of high dosage suramin treated rat TEM, ×2500

show a significant decrease in both measured parameters while high dosage suramin treated rats (group V) had a significantly decreased levels of BUN and SCr ($P < 0.05$) as compared to cisplatin group. However, no significant change ($P > 0.05$) was observed in both aforementioned parameters in the suramin alone treatment group (group II) as compared to control one.

Discussion

The kidneys are the major target for the toxic effects of various chemical agents owing to their high blood supply as they receive up to 25% of the cardiac output.[25] Drug nephrotoxicity was found to be responsible for 19% of acute kidney injury as reported in the epidemiological survey of critically ill patients.[26] Cisplatin nephrotoxicity developed primarily in the proximal tubules and its concentration in the RPTCs is 5 times higher than that of the serum, thus contributing to its toxicity.[27]

Researches on whether suramin has an effect on RPTCs after their damage by cisplatin are very limited and to our knowledge, no morphological and morphometrical study up till now has examined that effect. So, our goal was to determine whether suramin at different doses enhances morphological and morphometrical improvement of RPTCs after their damage by cisplatin.

In the present study, all results of suramin treated rats (group II) indicated its safety and nontoxicity as they were similar to the control one. Other researchers reported that the suramin at a dose of 0.1esent study, all results of suramin treated rats (group in mice after ischemia perfusion and that 10 mg/kg was not toxic.[14] Given the fact that concentration of suramin in the kidney is much higher than that of serum as it has a long half-life (21 days), so a one dose may achieve a therapeutic effect.[28]

Table 2: Number of caspase-3-immunopositive cells (N/1000 μm²) in control and experimental groups

Groups	Number of caspase-3-immunopositive cells (N/1000 μm²)
Group I	5.3±1.37
Group II	4.8±1.09
Group III	48.6±4.75[a]
Group IV	43.9±4.17
Group V	17.8±2.54[b]

Values are expressed as mean±SD. [a]$P<0.05$ as compared to control, [b]$P<0.05$ as compared to cisplatin group. SD: Standard deviation

Table 3: Blood urea nitrogen and serum creatinine levels (mg/dL) in control and experimental groups

Groups	BUN (mg/dL)	SCr (mg/dL)
Group I	21.8±2.21	0.51±0.014
Group II	20.05±2.19	0.49±0.03
Group III	76.4±3.1[a]	1.35±0.11[a]
Group IV	71.1±4.3	1.29±0.02
Group V	39.15±1.03[b]	0.71±0.46[b]

Values are expressed as mean±SD. [a]$P<0.05$ as compared to control, [b]$P<0.05$ as compared to cisplatin group. SD: Standard deviation

Our study revealed PCTs of cisplatin treated rats (group III) had various degenerative changes including loss of the cellular architecture, tubular lumen dilatation, brush border damage and marked vacuolated cytoplasm with pyknotic nuclei of the

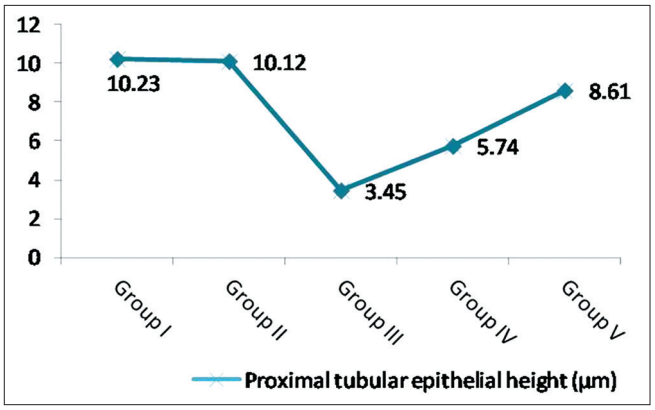

Graph 1: A significant reduction of proximal tubular epithelial height in group III in comparison to group I and a significant increasing in group V when compared with group III. Note nonsignificant change of epithelial height in group IV comparing with group III

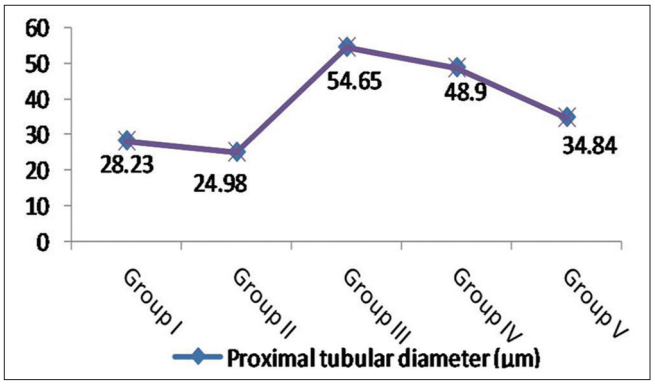

Graph 2: A significant increasing of proximal tubular diameter in group III in comparison to group I and a significant reduction in group V when compared with group III. Note nonsignificant change of tubular diameter in group IV comparing with group III

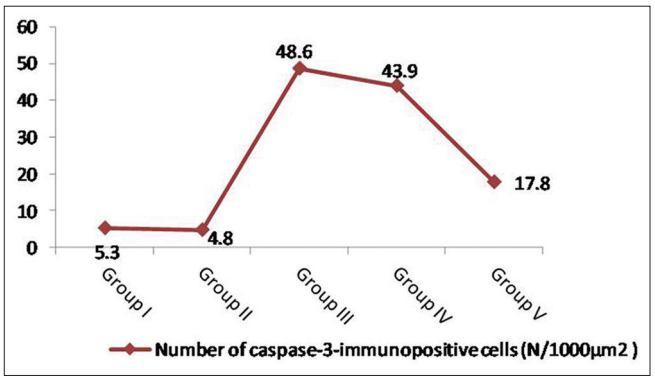

Graph 3: A significant increasing number of caspase-3-immunopositive cells in group III when compared with group I while it significantly decreased in group V comparing with group III. Note nonsignificant change of number of the cells in group IV comparing with group III

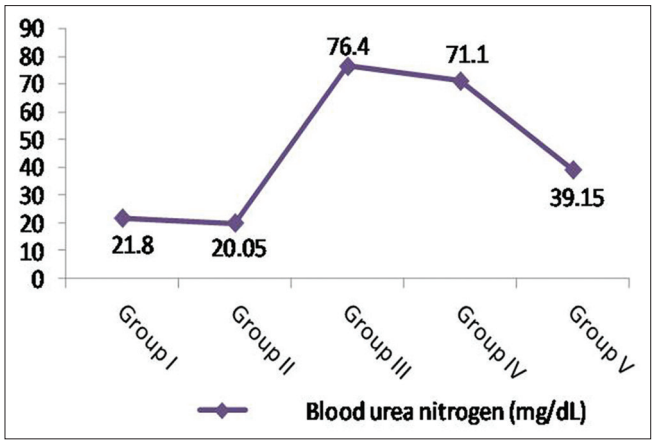

Graph 4: A significant increased blood urea nitrogen and serum creatinine in group III comparing with group I and a significant reduction of both parameters in group V comparing with group III. Note nonsignificant change of both parameters in group IV comparing with group III

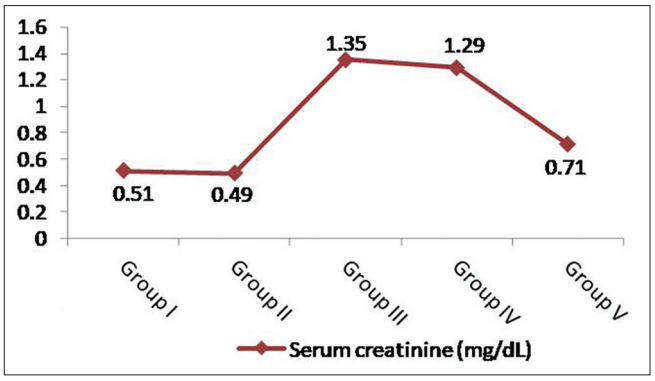

Graph 5: A significant increased blood urea nitrogen and serum creatinine in group III comparing with group I and a significant reduction of both parameters in group V comparing with group III. Note nonsignificant change of both parameters in group IV comparing with group III

RPTCs. Furthermore, TEM showed vacuolated destructed and small dense mitochondria as well as shrunken heterochromatic nuclei and interrupted basal lamina with its focal thickening. These results were confirmed morphometriclly that revealed a significant decrease of proximal tubular epithelium height associated with significantly increased tubular diameter compared with the control group. These results were consistent with those reported previously.[29-34] Moreover other investigators stated that cisplatin causes renal tubular toxicity without evident morphologic changes in glomeruli.[9,23]

Within the RPTCs, cisplatin is transformed into a highly reactive form that reacts rapidly with antioxidant molecules results in increased oxidative stress and ROM generation as well as lipid peroxidation production.[35] Consequently, the observed RPTCs desquamation into tubular lumen and tubular epithelium detachment may be related to damaged cell membranes as a result of production of ROM and lipid peroxidation. The intratubular hyaline casts might represent cellular debris combined with leakage precipitated proteins present in the tubular lumen.[33,36]

Preservation of brush border is very important for the function and survival of RPTCs that have been lost partially or completely after cisplatin injection as was shown by PAS reaction and confirmed utrastructurally. Previous researchers contributed this finding and the observable interrupted basal laminae to ROM generation which led to rapid loss of cytoskeletal integrity.[37]

The observed mononuclealar cellular infiltration after cisplatin injection was in consistence with other investigators[10,38,39] who reported that cisplatin evoked an inflammatory response with cell infiltration of renal tissue mainly mast cells, T cells, macrophages and neutrophils. It is well established both RPTCs and leukocytes have multiple P2 receptors that is playing an important role in increasing an inflammatory response through the realization of danger signals.[40,41] Furthermore, these receptors regulate the release of proinflammatory cytokines and chemokines molecules which attract and activate neutrophils to sites of damage, exacerbating the renal damage by potentiating an inflammatory response leading to the generation of ROM.[14,42]

In cisplatin treated rats ROM production leads to respiratory chain dysfunction as a result of mitochondrial DNA damage. Consequently the imbalance between oxidation and antioxidation leading to RPTCs damage and death.[43-45] Our data strongly supported that as the cisplatin induced sever alterations in mitochondrial shape and structure and this was consistence with other investigators.[32,46] Maintaining the orderly architecture of RPTCs and their basement membrane depends on the integration of nonoxidized lipids that have been lost after cisplatin treatment as a result of ROM formation with lipid peroxidation leading to lipid containing membranes dilation, suggesting cytoplasmic vacuolation and multiple heterogeneous vacuoles observed in this current study.

Furthermore, the results of previous study indicated that cytochrome P450 (CYP) 2E1 has an important role in cisplatin-induced RPTCs damage. This enzyme is localized to the RPTCs but not the glomeruli and is predominantly present in the endoplasmic reticulum. The interaction between cisplatin and CYP2E1 results in ROM generation and initiation of both RPTCs necrosis and apoptosis.[47]

There is growing evidence indicating RPTCs apoptosis increased the pathogenesis of cispaltin induced renal damage.[39,48,49] In the current study, the observed widespread positive caspase 3 immunoreactivity of cisplatin treated rats pointing to abundant apoptotic cells that was confirmed morphometrically as shown a significant increase in the number of caspase-3-positive cells. These results were in agreement with other study that reported involvement of cisplatin-induced tubular epithelial cells is in caspase-3 activation.[50]

Several apoptotic pathways are activated during cisplatin treatment including intrinsic and extrinsic one. The intrinsic pathway is associated with upregulation of mitochondrial permeability and caspase-3 activation by BAX as a result of

activation of a tumor suppressor P53,[50-52] while in the extrinsic one TNF-αNor other death receptor ligands may activate death receptors on the proximal tubular cell surface resulting in caspase-8 activation followed by downstream effector caspases such as caspase-3.[53,54]

In the current work the biochemical data of rats injected with cisplatin (group III) indicated impairment of renal function as there was a significance increase of both BUN and SCr. These data came hand by hand with histological and morphomertical results that could explain this disturbance. Impairment of the renal function is considered as a result of RPTCs damage as a consequence of ROM formation and it has been already reported by other studies.[34,47,55,56] In addition decreased glomerular filtration rate even if there is no glomerular damage can cause BUN and SCr elevations with subsequently aggravation of tubular damage.[57]

Comparing with cisplatin group, not low dosage treated suramin rats (group IV), but high dosage treated suramin one (group V) showed amelioration of toxic effects of cisplatin on RPTCs. Low dosage suramin failed to improve the morphological changes of the RPTCs as well as the widespread positive caspase immunoreactivity induced by cispaltin while, high dosage suramin resulted in partial morphological RPTCs improvement associated with weak caspase immunoreactivity. Electron microscopic results supported these findings that revealed appearance of RPTCs with large euchromatic nuclei, numerous intact elongated mitochondria and restoration of most cells to their normal structures than those observed in low dosage suramin group.

Suramin acts on oxidative formation downstream and its effect as a pan P2 receptor antagonist attenuates expression of the proinflammatory factors as cytokines and consequently protects RPTCs from the inflammatory response and oxidative stress associated with cisplatin nephrotoxicity.[58-60] In addition, previous study found that inhibition of mast cell degranulation in mice after cisplatin treatment with subsequently decreasing the release of cytokine TNF-αNfrom RPTCs dampened the proinflammatory response and further attenuated its toxicity.[61]

Moreover, the observed morphometric results confirmed the histological one as Low dosage suramin showed no significant changes in both the proximal tubular epithelial height and tubular diameter as well as the caspase-3-immunopositive cells that remained significantly high compared with cisplatin group. In contrast high dosage suramin was able to significantly decrease the caspase-3-immunopositive cells and showed significant proximal tubular epithelial height increasing and tubular diameter decreasing.

Consistent with our results, previous researchers[14] found that suramin attenuated renal tubular damage and decreased the number of apoptotic cells of proximal tubules in ischemic reperfusion injured kidneys. The possibility of antiapotptotic effect of suramin may be through blocking death receptor activation on RPTCs as apoptosis is mediated by TNF-αNleading to reducing caspases activation, decreasing endoplasmic reticulum stress induced apoptosis and preventing mitochondrial membrane potential loss.[16] The observed intact mitochondria in group V with subsequently reducing caspases activation and cytochrome C release are important factors for RPTCs survival and function.

In the current work, the improvement of renal function by suramin occurred in a dose-dependent manner in concomitant with histological and morphometrical results. The biochemical data showed the rats treated with high dosage suramin but not a lower one improved the cisplatin-induced decreased in kidney function. There was a significance increased in both parameters (BUN and SCr) that indicated the morphological RPTCs improvement. It was found that suramin accelerates renal function recovery after acute kidney injury as it promotes RPTCs proliferation *in vitro* and *in vivo* and through interference of late-onset apoptosis.[14]

Interestingly, previous data revealed suramin induced renal growth in rats, predominantly in the RPTCs with no glomeruli alterations through Src-dependent activation of the PI3K/Akt pathway. These two important signaling molecules (Src and Akt) are associated with cell survival and proliferation, may mediate recovery of renal function through this mechanism.[59] Moreover, an increased number of intact mitochondria of RPTCs that were noted in group V may reflect compensatory adaptation to produce much energy to improve the renal function.

Conclusion

The present study showed that simultaneous administration of suramin to the cisplatin-treated rats abrogates the toxic effect of cisplatin on RPTCs in a dosage-dependent manner. High dosage suramin has a potential renoprotective effect at both morphological and morphometrical levels as well as restores renal function to normal one.

Financial support and sponsorship

Nil.

Conflicts of interest

There are no conflicts of interest.

References

1. World Health Organization. Cancer. World Health Organization; 2018. Available from: http://www.who.int/news-room/fact sheets/detail/cancer. [Last accessed on 2018 Feb 01].
2. Marcato PD, Fávaro WJ, Durán N. Cisplatin properties in a nanobiotechnological approach to cancer: A mini-review. Curr Cancer Drug Targets 2014;14:458-76.
3. Liu X, Huang Z, Zou X, Yang Y, Qiu Y, Wen Y. Panax notoginseng saponins attenuates cisplatin-induced nephrotoxicity via inhibiting the mitochondrial pathway of apoptosis. Int J Clin Exp Pathol 2014;7:8391-400.
4. Okuma Y, Saito M, Hosomi Y, Sakuyama T, Okamura T. Key components of chemotherapy for thymic malignancies: A systematic review and pooled analysis for anthracycline-, carboplatin- or cisplatin-based chemotherapy. J Cancer Res Clin Oncol 2015;141:323-31.
5. Jia Z, Wang N, Aoyagi T, Wang H, Liu H, Yang T. Amelioration of cisplatin nephrotoxicity by genetic or pharmacologic blockade of

prostaglandin synthesis. Kidney Int 2011;79:77-88.
6. Jiménez-Triana CA, Castelán-Martínez OD, Rivas-Ruiz R, Jiménez-Méndez R, Medina A, Clark P, *et al.* Cisplatin nephrotoxicity and longitudinal growth in children with solid tumors: A retrospective cohort study. Medicine (Baltimore) 2015;94:e1413.
7. Kimura T, Nojiri T, Hosoda H, Ishikane S, Shintani Y, Inoue M, *et al.* Protective effects of C-type natriuretic peptide on cisplatin-induced nephrotoxicity in mice. Cancer Chemother Pharmacol 2015;75:1057-63.
8. Price PM, Yu F, Kaldis P, Aleem E, Nowak G, Safirstein RL, *et al.* Dependence of cisplatin-induced cell death *in vitro* and *in vivo* on cyclin-dependent kinase 2. J Am Soc Nephrol 2006;17:2434-42.
9. Yao X, Panichpisal K, Kurtzman N, Nugent K. Cisplatin nephrotoxicity: A review. Am J Med Sci 2007;334:115-24.
10. Miller RP, Tadagavadi RK, Ramesh G, Reeves WB. Mechanisms of cisplatin nephrotoxicity. Toxins (Basel) 2010;2:2490-518.
11. Pabla N, Dong Z. Cisplatin nephrotoxicity: Mechanisms and renoprotective strategies. Kidney Int 2008;73:994-1007.
12. Liu N, Zhuang S. Tissue protective and anti-fibrotic actions of suramin: New uses of an old drug. Curr Clin Pharmacol 2011;6:137-42.
13. Berthier CC, Zhang H, Schin M, Henger A, Nelson RG, Yee B, *et al.* Enhanced expression of Janus kinase-signal transducer and activator of transcription pathway members in human diabetic nephropathy. Diabetes 2009;58:469-77.
14. Zhuang S, Lu B, Daubert RA, Chavin KD, Wang L, Schnellmann RG. Suramin promotes recovery from renal ischemia/reperfusion injury in mice. Kidney Int 2009;75:304-11.
15. Liu N, Tolbert E, Ponnusamy M, Yan H, Zhuang S. Delayed administration of suramin attenuates the progression of renal fibrosis in obstructive nephropathy. J Pharmacol Exp Ther 2011;338:758-66.
16. Eichhorst ST, Krueger A, Müerköster S, Fas SC, Golks A, Gruetzner U, *et al.* Suramin inhibits death receptor-induced apoptosis *in vitro* and fulminant apoptotic liver damage in mice. Nat Med 2004;10:602-9.
17. Song S, Wientjes MG, Walsh C, Au JL. Nontoxic doses of suramin enhance activity of paclitaxel against lung metastases. Cancer Res 2001;61:6145-50.
18. Xi JX, Liu XX, Yang YF, Zhang CH, Liu HG. Effect of xueshuantong on renal function and oxidation indexes in cisplatin-induced nephroxicity rats. Chin J Exp Tradit Med Form 2012;18:263-6.
19. Mashhadi MA, Arab MR, Azizi F, Shahraki MR. Histological study of toxic effects of cisplatin single dose injection on rat kidney. Gene Cell Tissue 2014;1:e21536.
20. Bancroft JD, Layton C. The hematoxylin and eosin. In: Suvarna SK, Layton C, Bancroft JD, editors. Bancroft's Theory & Practice of Histological Techniques. 7th ed., Ch. 10. Philadelphia: Churchill Livingstone of Elsevier; 2013. p. 172-86.
21. Jackson P, Blythe D. Immunohistochemical techniques. In: Suvarna SK, Layton C, Bancroft JD, editors. Bancroft's Theory & Practice of Histological Techniques. 7th ed., Ch. 18. Philadelphia: Churchill Livingstone of Elsevier; 2013. p. 381-434.
22. Kamada S, Kikkawa U, Tsujimoto Y, Hunter T. Nuclear translocation of caspase-3 is dependent on its proteolytic activation and recognition of a substrate-like protein(s). J Biol Chem 2005;280:857-60.
23. Ayache J, Beaunier L, Boumendil J, Ehret G, Laub D. Sample Preparation Handbook for Transmission Electron Microscopy Techniques. New York/Dordrecht/Heidelberg/London: Springer; 2010.
24. Traynor J, Mactier R, Geddes CC, Fox JG. How to measure renal function in clinical practice. BMJ 2006;333:733-7.
25. Pujalté I, Passagne I, Brouillaud B, Tréguer M, Durand E, Ohayon-Courtès C, *et al.* Cytotoxicity and oxidative stress induced by different metallic nanoparticles on human kidney cells. Part Fibre Toxicol 2011;8:10.
26. Uchino S, Kellum JA, Bellomo R, Doig GS, Morimatsu H, Morgera S, *et al.* Acute renal failure in critically ill patients: A multinational, multicenter study. JAMA 2005;294:813-8.
27. Kodama A, Watanabe H, Tanaka R, Kondo M, Chuang VT, Wu Q, *et al.* Albumin fusion renders thioredoxin an effective anti-oxidative and anti-inflammatory agent for preventing cisplatin-induced nephrotoxicity. Biochim Biophys Acta 2014;1840:1152-62.
28. McNally WP, DeHart PD, Lathia C, Whitfield LR. Distribution of [14C] suramin in tissues of male rats following a single intravenous dose. Life Sci 2000;67:1847-57.
29. Vickers AE, Rose K, Fisher R, Saulnier M, Sahota P, Bentley P. Kidney slices of human and rat to characterize cisplatin-induced injury on cellular pathways and morphology. Toxicol Pathol 2004;32:577-90.
30. Fouad AA, Morsy MA, Gomaa W. Protective effect of carnosine against cisplatin-induced nephrotoxicity in mice. Environ Toxicol Pharmacol 2008;25:292-7.
31. Jariyawat S, Kigpituck P, Suksen K, Chuncharunee A, Chaovanalikit A, Piyachaturawat P. Protection against cisplatin-induced nephrotoxicity in mice by curcuma comosa roxb. Ethanol extract. J Nat Med 2009;63:430-6.
32. Yousef MM, Helal OK, Adly N. Effect of silymarin on cisplatin-induced renal tubular injuries in adult male rabbits: a histological, immunohistochemical, and electron microscopic study. Egypt J Histol 2011;34:800-7.
33. Liang H, Liu HZ, Wang HB, Zhong JY, Yang CX, Zhang B. Dexmedetomidine protects against cisplatin-induced acute kidney injury in mice through regulating apoptosis and inflammation. Inflamm Res 2017;66:399-411.
34. Ashraf YN. Effect of misoprostol on ultrastructural changes of renal tissues in cisplatin-treated adult rats. J Cytol Histol 2013;4:1-7.
35. Aydinoz S, Uzun G, Cermik H, Atasoyu EM, Yildiz S, Karagoz B, *et al.* Effects of different doses of hyperbaric oxygen on cisplatin-induced nephrotoxicity. Ren Fail 2007;29:257-63.
36. Metawe SM, Naim MM, El Wazir YM, Saleh SA. Histological study on the effect of haematopoietic stem cells on the adriamycin model of nephropathy in albino rats. Egypt J Histol 2011;34:448-58.
37. Sadek EM, Salama NM, Ismail DI, Elshafei AA. Histological study on the protective effect of endogenous stem-cell mobilization in Adriamycin-induced chronic nephropathy in rats. J Microsc Ultrastruct 2016;4:133-42.
38. Faubel S, Lewis EC, Reznikov L, Ljubanovic D, Hoke TS, Somerset H, *et al.* Cisplatin-induced acute renal failure is associated with an increase in the cytokines interleukin (IL)-1beta, IL-18, IL-6, and neutrophil infiltration in the kidney. J Pharmacol Exp Ther 2007;322:8-15.
39. Ozkok A, Edelstein CL. Pathophysiology of cisplatin-induced acute kidney injury. Biomed Res Int 2014;2014:967826.
40. Unwin RJ, Bailey MA, Burnstock G. Purinergic signaling along the renal tubule: The current state of play. News Physiol Sci 2003;18:237-41.
41. Chen J, Zhao Y, Liu Y. The role of nucleotides and purinergic signaling in apoptotic cell clearance – Implications for chronic inflammatory diseases. Front Immunol 2014;5:656.
42. Braganhol E, Kukulski F, Lévesque SA, Fausther M, Lavoie EG, Zanotto-Filho A, *et al.* Nucleotide receptors control IL-8/CXCL8 and MCP-1/CCL2 secretions as well as proliferation in human glioma cells. Biochim Biophys Acta 2015;1852:120-30.
43. Kruidering M, Van de Water B, de Heer E, Mulder GJ, Nagelkerke JF. Cisplatin-induced nephrotoxicity in porcine proximal tubular cells: Mitochondrial dysfunction by inhibition of complexes I to IV of the respiratory chain. J Pharmacol Exp Ther 1997;280:638-49.
44. Lebrecht D, Setzer B, Rohrbach R, Walker UA. Mitochondrial DNA and its respiratory chain products are defective in doxorubicin nephrosis. Nephrol Dial Transplant 2004;19:329-36.
45. Turrens JF. Mitochondrial formation of reactive oxygen species. J Physiol 2003;552:335-44.
46. Mahdy AA, El-Morshdy KE. Role of losartan on the renal cortex damage induced by cisplatin in adult male albino rats. Egypt J Histol 2014;37:480-91.
47. Liu H, Baliga R. Cytochrome P450 2E1 null mice provide novel protection against cisplatin-induced nephrotoxicity and apoptosis. Kidney Int 2003;63:1687-96.
48. Ramesh G, Reeves WB. TNFR2-mediated apoptosis and necrosis in cisplatin-induced acute renal failure. Am J Physiol Renal Physiol 2003;285:F610-8.
49. Nozaki Y, Kinoshita K, Hino S, Yano T, Niki K, Hirooka Y, *et al.* Signaling Rho-kinase mediates inflammation and apoptosis in T cells and renal tubules in cisplatin nephrotoxicity. Am J Physiol Renal Physiol 2015;308:F899-909.
50. Bolisetty S, Traylor A, Joseph R, Zarjou A, Agarwal A. Proximal

tubule-targeted heme oxygenase-1 in cisplatin-induced acute kidney injury. Am J Physiol Renal Physiol 2016;310:F385-94.
51. Lee RH, Song JM, Park MY, Kang SK, Kim YK, Jung JS. Cisplatin-induced apoptosis by translocation of endogenous bax in mouse collecting duct cells. Biochem Pharmacol 2001;62:1013-23.
52. Jiang M, Yi X, Hsu S, Wang CY, Dong Z. Role of p53 in cisplatin-induced tubular cell apoptosis: Dependence on p53 transcriptional activity. Am J Physiol Renal Physiol 2004;287:F1140-7.
53. Dhanasekaran DN, Reddy EP. JNK signaling in apoptosis. Oncogene 2008;27:6245-51.
54. Brenner D, Blaser H, Mak TW. Regulation of tumour necrosis factor signalling: Live or let die. Nat Rev Immunol 2015;15:362-74.
55. Khoshnoud MJ, Naji B, Moghbela A, Geramizadehb B, Niknahada H. Effect of simvastatin on cisplatin-induced nephrotoxicity in male rats. Iran J Pharm Sci 2011;7:165-73.
56. Ali DA, Abdeen AM, Ismail MF, Mostafa MA. Histological, ultrastructural and immunohistochemical studies on the protective effect of ginger extract against cisplatin-induced nephrotoxicity in male rats. Toxicol Ind Health 2015;31:869-80.
57. Mingeot-Leclercq MP, Tulkens PM. Aminoglycosides: Nephrotoxicity. Antimicrob Agents Chemother 1999;43:1003-12.
58. Jenkinson KM, Reid JJ. The P(2)-purinoceptor antagonist suramin is a competitive antagonist at vasoactive intestinal peptide receptors in the rat gastric fundus. Br J Pharmacol 2000;130:1632-8.
59. Zhuang S, Schnellmann RG. Suramin promotes proliferation and scattering of renal epithelial cells. J Pharmacol Exp Ther 2005;314:383-90.
60. He S, Rehman H, Shi Y, Krishnasamy Y, Lemasters JJ, Schnellmann RG, *et al.* Suramin decreases injury and improves regeneration of ethanol-induced steatotic partial liver grafts. J Pharmacol Exp Ther 2013;344:417-25.
61. Summers SA, Chan J, Gan PY, Dewage L, Nozaki Y, Steinmetz OM, *et al.* Mast cells mediate acute kidney injury through the production of TNF. J Am Soc Nephrol 2011;22:2226-36.